Binding energies of shallow impurities in asymmetric strained wurtzite $Al_xGa_{1-x}N$/GaN/$Al_yGa_{1-y}N$ quantum wells*

Ha Sihua(哈斯花)[1,†], Ban Shiliang(班士良)[2], and Zhu Jun(朱俊)[2]

[1]Department of Physics, College of Sciences, Inner Mongolia University of Technology, Hohhot 010051, China
[2]School of Physical Science and Technology, Inner Mongolia University, Hohhot 010021, China

Abstract: The ground state binding energies of hydrogenic impurities in strained wurtzite $Al_xGa_{1-x}N$/GaN/$Al_yGa_{1-y}N$ quantum wells are calculated numerically by a variational method. The dependence of the binding energy on well width, impurity location and Al concentrations of the left and right barriers is discussed, including the effect of the built-in electric field induced by spontaneous and piezoelectric polarizations. The results show that the change in binding energy with well width is more sensitive to the impurity position and barrier heights than the barrier widths, especially in asymmetric well structures where the barrier widths and/or barrier heights differ. The binding energy as a function of the impurity position in symmetric and asymmetric structures behaves like a map of the spatial distribution of the ground state wave function of the electron. It is also found that the influence on the binding energy from the Al concentration of the left barrier is more obvious than that of the right barrier.

Key words: quantum well; impurity; strain; polarization
DOI: 10.1088/1674-4926/32/4/042001 **PACC:** 7320D; 7155F; 4210N

1. Introduction

In recent years, a great deal of interest has been devoted to the study of the impurity states in modulation-doped quantum well structures which have been widely used in high-speed electronic devices. Some authors[1−4] adopted a variational method to calculate the ground state binding energies of hydrogenic impurities in closely lattice matched GaAs/$Al_xGa_{1-x}As$ quantum wells (QW) as functions of the well width and Al concentration. They showed that the binding energies of impurities, which are always assumed to be located at the center of quantum well, are increased as expected by increasing the Al concentration. On the other hand, a large group of authors also paid attention to the problem of an off-center impurity and obtained the change in binding energy with impurity position by choosing a fixed well[5−9].

In the case of strained wurtzite GaN/AlGaN QW heterostructures, the effect of a large built-in electric field on the physical properties of these structures has attracted considerable interest[10−12]. As is known, the built-in electric field is produced by the spontaneous and strain-induced piezoelectric polarizations. It can change the band structures of QWs and then shift the energy levels of carriers. Morel *et al*.[10] presented a calculation of the donor binding energy in GaN/$Al_xGa_{1-x}N$ QWs, including the effect of internal electric field. The variations in binding energy versus well width and impurity position are compared with and without built-in electric field. By considering the interaction of electrons and impurities with phonons, Shi *et al*.[11, 12] investigated theoretically the effects of built-in field on ionization energy of a bound polaron in GaN/AlN QWs and also found that the built-in field has a considerable influence on polaron energies. However, the intensity of the field is taken as a constant $F = 9.4$ MV/cm. In fact, the value of the field depends strongly on the thickness and Al concentration of each layer[13]. It should be pointed out that almost all of the authors ignored the discussion of the effects of surrounding barriers. They always chose the height and width of each barrier as equal or assumed them to be infinite.

In this paper, the binding energy of shallow donor impurities in modulation-doped strained wurtzite $Al_xGa_{1-x}N$/GaN/$Al_yGa_{1-y}N$ QWs with different well and barrier widths, as well as different Al concentrations in barrier layers, has been investigated.

2. Donor binding energy

We consider an $Al_xGa_{1-x}N$/GaN/$Al_yGa_{1-y}N$ strained QW with finite barriers to calculate the binding energies of shallow donor impurities. The potential profile is given in Fig. 1. The z axis is taken to be parallel to the c axis and the x–y plane parallel to the interfaces. The coordinate origin is chosen as the center of the well. Within the framework of effective mass and single-band approximations, the Hamiltonian for an electron bound to a hydrogenic impurity can be written as

$$H_{\rm d} = -\frac{\hbar^2}{2m_{\rm e}^{//}}\frac{1}{\rho}\frac{\partial}{\partial\rho}\rho\frac{\partial}{\partial\rho} - \frac{\hbar^2}{2}\frac{\partial}{\partial z}\left[\frac{1}{m_{\rm e}^{\perp}(z)}\right]\frac{\partial}{\partial z} + V(z) + eF(z)z - \frac{e^2}{4\pi\varepsilon_0\varepsilon(z,z_0)\sqrt{\rho^2+(z-z_0)^2}}, \quad (1)$$

* Project supported by the National Natural Science Foundation of China (No. 60966001), the Specialized Research Fund for the Doctoral Program of Higher Education of China (No. 20070126001), the Key Project of Natural Science Foundation of Inner Mongolia Autonomous Region (No. 20080404Zd02), and the Doctoral Science Foundation of Inner Mongolia Autonomous Region (No. 2010BS0102).
† Corresponding author. Email: hasihua_121@163.com
Received 10 September 2010, revised manuscript received 18 October 2010

where $m_e^{\perp}$ and $m_e^{//}$ are the effective masses of the electron parallel and perpendicular to the z direction, V is the barrier height[14] and F is the built-in electric field. ρ is the radial component of the electron coordinate in the x–y plane. $\varepsilon(z, z_0)$ is the static dielectric constant related to the position of the electron and the impurity.

The Schrödinger equation for a free electron in the z direction can be written as

$$\left\{-\frac{\hbar^2}{2}\frac{\partial}{\partial z}\left[\frac{1}{m_e^{\perp}(z)}\right]\frac{\partial}{\partial z}+V(z)+eF(z)z\right\}\psi(z)=E\psi(z). \tag{2}$$

The electron energy level E and wave function $\psi(z)$ can be obtained simultaneously via a numerical procedure.

A one-parameter trial wave function in the x–y plane is used to calculate the variational energy of the impurity state. It follows as

$$\psi(\rho)=\sqrt{\frac{1}{2\pi}}\lambda \mathrm{e}^{-\frac{\lambda}{2}\rho}, \tag{3}$$

where λ is the variational parameter.

Combining Eqs. (1) and (2) with Eq. (3), the variational energy of the ground state impurity can be written as

$$E_d(\lambda)=\langle\psi(\rho)|\langle\psi(z)|H_d|\psi(z)\rangle|\psi(\rho)\rangle. \tag{4}$$

As a result, the binding energy of the ground state impurity can be written as

$$E_b=E_{free}-\min_{\lambda}E_d(\lambda), \tag{5}$$

where E_{free} is the ground state energy of the free electron, which can be obtained by repeating the above process but removing the Coulomb potential in Eq. (1) and replacing Eq. (3) by a plane wave function.

3. Strain effect

The modification of the strain effect on material parameters, such as the energy gap, effective mass of electron, dielectric constant and polarization field, is taken into account.

In the well and barrier, the biaxial lattice-mismatch induced strains are given by

$$\kappa_{xx,j}=\kappa_{yy,j}=\frac{a_{eq}-a_j}{a_j}. \tag{6}$$

From Hooke's law, the uniaxial and biaxial strain tensor ratio can be expressed by

$$\frac{\kappa_{zz,j}}{\kappa_{xx,j}}=\frac{c_{11,j}+c_{12,j}-2c_{13,j}}{c_{33,j}-c_{13,j}}. \tag{7}$$

In Eqs. (6) and (7), the subscripts j = w, lb and rb denote the well, left barrier and right barrier, a_j is the unstrained lattice constant of the j-layer material. c_{11}, c_{12}, c_{13} and c_{33} are the elastic constants. a_{eq} is the equilibrium lattice constant shared by all of the layers, which can be written as[15]

$$a_{eq}=\frac{a_wD_wG_w+a_{lb}D_{lb}G_{lb}+a_{rb}D_{rb}G_{rb}}{D_wG_w+D_{lb}G_{lb}+D_{rb}G_{rb}}, \tag{8}$$

in which D_j is the width of the j-layer. G_j can be obtained from

$$G_j=2(c_{11,j}+c_{12,j}-2c_{13,j}^2/c_{33,j}). \tag{9}$$

Modified by the strain effect, the energy gaps of each layer material are given as[16]

$$E_{g,j}=E_{g,j}^0+[d_{1,j}+b_{1,j}]2\kappa_{xx,j}+[d_{2,j}+b_{2,j}]\kappa_{zz,j}, \tag{10}$$

where $d_{1,j}$, $d_{2,j}$, $b_{1,j}$ and $b_{2,j}$ are the deformation potentials in the j-layer. For the ternary mixed crystal $Al_xGa_{1-x}N$ (chosen as the left barrier) and $Al_yGa_{1-y}N$ (chosen as the right barrier), the energy gap is given as

$$E_{g,lb(Al_xGa_{1-x}N)}=xE_{g,(GaN)}+(1-x)E_{g,(AlN)}-bx(1-x), \tag{11}$$

$$E_{g,rb(Al_yGa_{1-y}N)}=yE_{g,(GaN)}+(1-y)E_{g,(AlN)}-by(1-y), \tag{12}$$

where b is the band-gap bowing coefficient, which is taken as 0.612 eV[17].

The biaxial and uniaxial strain dependences of the effective masses of an electron in the z direction and the x–y plane can be calculated by

$$\frac{m_e^{\perp,//}}{m_0}=\left(1+\frac{E_p^{\perp,//}}{E_g}\right)^{-1}, \tag{13}$$

where $E_p^{\perp,//}$ is the $k\cdot p$ interaction energy defined in Ref. [18].

Otherwise, the static dielectric constant is also influenced by the biaxial and uniaxial strain effect. It can be derived from the Lyddane–Sachs–Teller relation

$$\varepsilon_j^{\perp,//}=\varepsilon_{\infty,j}^{\perp,//}\left(\frac{\omega_{LO,j}^{\perp,//}}{\omega_{TO,j}^{\perp,//}}\right)^2, \tag{14}$$

where the frequencies of LO- and TO-phonons influenced by strain can be written as[16]

$$\omega_{LO,TO,j}^{\perp,//}=\omega_{LO,TO,j}^{0\perp,//}+K_{xx,j}2\kappa_{xx,j}+K_{zz,j}\kappa_{zz,j}, \tag{15}$$

where $K_{xx,j}$ and $K_{zz,j}$ are the strain coefficients of phonon modes given in Ref. [16].

The built-in electric field F due to the spontaneous and piezoelectric polarizations is different in the well and barriers. It follows as [13]

$$F_w=\frac{\varepsilon_{0,w}^{\perp}\varepsilon_{0,lb}^{\perp}D_{rb}(P_{rb}^{tot}-P_w^{tot})+\varepsilon_{0,w}^{\perp}\varepsilon_{0,rb}^{\perp}D_{lb}(P_{lb}^{tot}-P_w^{tot})}{\varepsilon_{0,w}^{\perp\,2}(\varepsilon_{0,lb}^{\perp}D_{rb}+\varepsilon_{0,rb}^{\perp}D_{lb})+\varepsilon_{0,w}^{\perp}\varepsilon_{0,lb}^{\perp}\varepsilon_{0,rb}^{\perp}D_w}, \tag{16}$$

$$F_{lb}=\frac{\varepsilon_{0,w}^{\perp\,2}D_{rb}(P_{rb}^{tot}-P_{lb}^{tot})+\varepsilon_{0,w}^{\perp}\varepsilon_{0,rb}^{\perp}D_w(P_w^{tot}-P_{lb}^{tot})}{\varepsilon_{0,w}^{\perp\,2}(\varepsilon_{0,lb}^{\perp}D_{rb}+\varepsilon_{0,rb}^{\perp}D_{lb})+\varepsilon_{0,w}^{\perp}\varepsilon_{0,lb}^{\perp}\varepsilon_{0,rb}^{\perp}D_w}, \tag{17}$$

$$F_{rb}=\frac{\varepsilon_{0,w}^{\perp\,2}D_{lb}(P_{lb}^{tot}-P_{rb}^{tot})+\varepsilon_{0,w}^{\perp}\varepsilon_{0,lb}^{\perp}D_w(P_w^{tot}-P_{rb}^{tot})}{\varepsilon_{0,w}^{\perp\,2}(\varepsilon_{0,lb}^{\perp}D_{rb}+\varepsilon_{0,rb}^{\perp}D_{lb})+\varepsilon_{0,w}^{\perp}\varepsilon_{0,lb}^{\perp}\varepsilon_{0,rb}^{\perp}D_w}, \tag{18}$$

where the fields in three layers satisfy the periodic boundary condition $\sum_{j=w,lb,rb}F_jD_j=0$. Here, the total polarization in each layer is

$$P_j^{tot}=P_j^{sp}+P_j^{pz}. \tag{19}$$

P_j^{sp} is the spontaneous polarization, and the piezoelectric polarization P_j^{pz} is given as[13]

$$P_j^{pz}=2e_{31,j}\kappa_{xx,j}+e_{33,j}\kappa_{zz,j}. \tag{20}$$

Here, $e_{31,j}$ and $e_{33,j}$ are the piezoelectric constants.

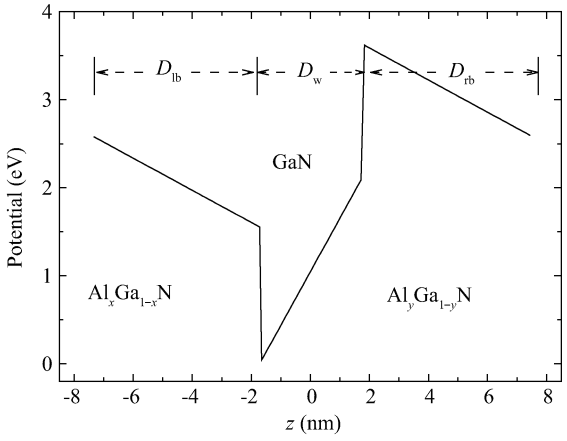

Fig. 1. Conduction band edge profile of an $Al_xGa_{1-x}N/GaN/Al_yGa_{1-y}N$ QW.

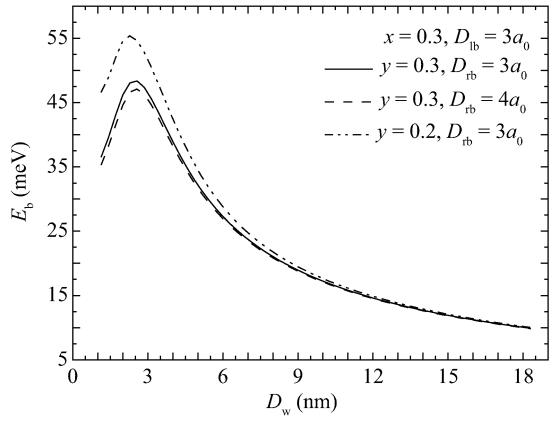

Fig. 2. Binding energy E_b as a function of the well width D_w for the impurity located at the center of the well. The Al concentration and barrier width of the left barrier are fixed as 0.3 and $3a_0$. The solid, dashed and dot-dashed curves represent $y = 0.3$, $D_{rb} = 3a_0$, $y = 0.3$, $D_{rb} = 4a_0$, and $y = 0.2$, $D_{rb} = 3a_0$, respectively.

4. Results and discussion

The calculated results are shown in Figs. 2–6.

The binding energy E_b as a function of the well width D_w for the impurity located at the center of the well with fixed Al concentration and barrier width of the left barrier is depicted in Fig. 2. It can be seen that E_b first increases slowly to reach a maximum, then decreases with decreasing well width in all three cases. If the barriers are not symmetric, the influence on E_b from the variation of the width of the right barrier is obviously less than from the Al concentration, especially when the well is narrower. This is due to the penetration of the electron wave function into the right barrier. Although the electron wave function mainly locates in the left region of the well due to the strong built-in electric field in the structure, it can penetrate a little into the right barrier layer because of the opposite field in the barriers. But the depth of penetration is still small. That is to say, the effect on E_b from the width of the right barrier is comparably small. As the Al concentration of the right barrier decreases, the corresponding potential height falls, and then the wave function can easily penetrate into the right barrier

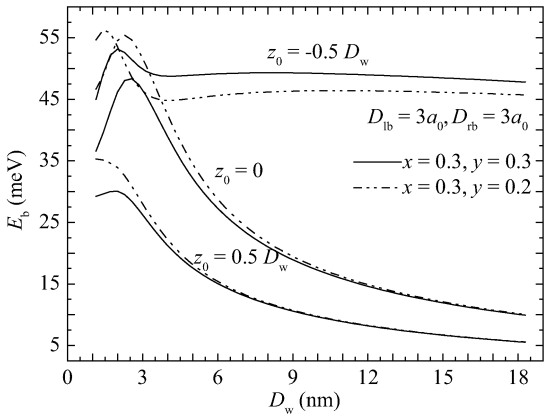

Fig. 3. Binding energy E_b as a function of the well width D_w for the given barrier widths $D_{lb} = D_{rb} = 3a_0$ and impurity position $z_0 = -0.5D_w$, $z_0 = 0$ and $z_0 = 0.5D_w$. The solid, dot-dashed curves represent $x = 0.3$, $y = 0.3$ and $x = 0.3$, $y = 0.2$ respectively.

resulting in an increase in E_b. However, when the well width is much larger, the electron wave function hardly penetrates into the barriers and the influence from the variation of barriers can be ignored.

We also plot the binding energy as a function of the well width D_w when the impurity is located in different position in Fig. 3. It is found that two curves are qualitatively same for the impurity position $z_0 = 0$ and $z_0 = 0.5D_w$. However, the value of E_b for the impurity located at the right interface is weaker, especially in the narrower QW due to the larger average distance between the electron and the impurity. As the Al concentration of the right barrier decreases, the potential height decreases correspondingly and E_b increases in both cases. This is because of more penetration of the electron wave function to the right barrier. If the impurity locates at the left interface of the structure, E_b hardly changes as the well width becomes much larger and the values of E_b are larger than those in the previous two conditions. However, E_b for the impurity located at the left interface in QW with $x > y$ is smaller than that with $x = y$ for a large value of the well widths. When the well becomes wider, the probability of finding an electron on the right side of the QW increases, then E_b decreases.

As seen in Fig. 4, the impurity binding energy E_b as a function of the impurity position z_0 behaves like a map of the spatial distribution of the ground state wave function of the electron. As the impurity shifts to the barrier region, the value of E_b becomes smaller since the Coulomb interaction between the electron and the impurity weakens. It is also found that the maximum point of E_b moves forward to the left side of the well because the built-in electric field compels the electron to shift to the left from the center of the well. When the Al concentration of left barrier is less than that of the right barrier, E_b decreases due to the greater probability of finding the electron in the left barrier layer.

The influence of the Al concentration of different barriers on the impurity binding energy E_b is shown in Figs. 5 and 6. One can observe that the variation in E_b is dramatically dependent on the impurity position. When $z_0 = 0$ and $0.5D_w$, E_b decreases with increasing Al concentration of the right barrier,

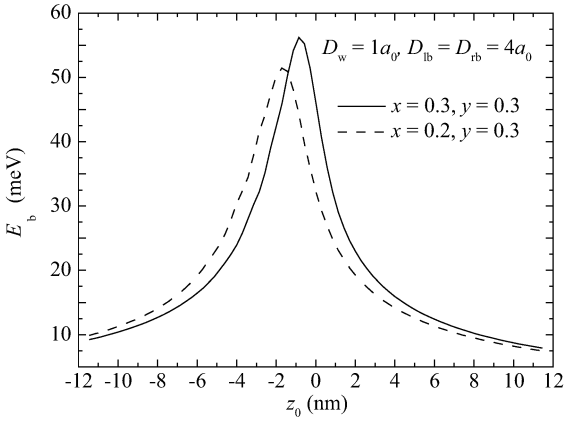

Fig. 4. Binding energy E_b as a function of the impurity position z_0 for $D_w = a_0$ and $D_{lb} = D_{rb} = 4a_0$. The solid, dashed curves represent $x = 0.3$, $y = 0.3$ and $x = 0.2$, $y = 0.3$ respectively.

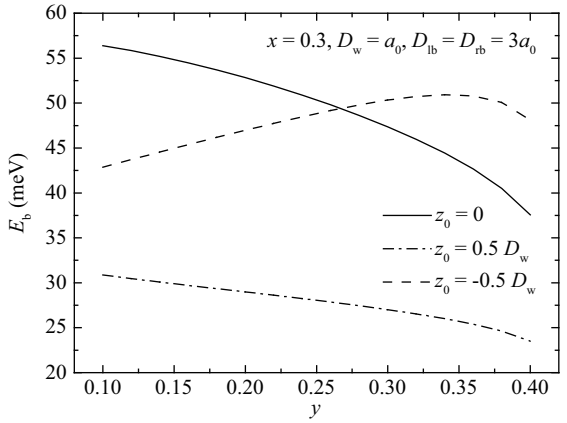

Fig. 5. Binding energy E_b as a function of the Al concentration of the right barrier y for $x = 0.3$, $D_w = a_0$ and $D_{lb} = D_{rb} = 3a_0$. The solid, dashed and dot-dashed curves represent $z_0 = 0$, $z_0 = -0.5D_w$ and $z_0 = 0.5D_w$, respectively.

while it increases with increasing Al concentration of the left barrier. When $z_0 = -0.5D_w$, E_b increases as the Al concentration increases in both cases. This is attributed to the distribution of the electron wave function and the average distance between the electron and the impurity. Due to the strong built-in electric field, the electron wave function almost resides near the left interface and more easily penetrates into the left barrier. Therefore, E_b is more sensitive to the Al concentration of the left barrier and the distance of the impurity from the left interface. It is evident that E_b is determined not only by the quantum confinement of the well structure but also by the strong built-in electric field which makes the Coulomb interaction stronger or weaker decided by the relative position of the electron and the impurity.

5. Summary

We have performed a variational calculation of the ground state binding energies of hydrogenic impurities in strained wurtzite $Al_xGa_{1-x}N/GaN/Al_yGa_{1-y}N$ QWs by taking the built-in electric field into account. The results show that the

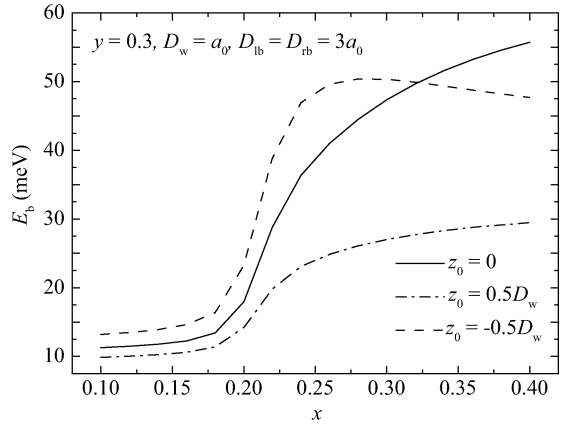

Fig. 6. Binding energy E_b as a function of the Al concentration of the left barrier x for $y = 0.3$, $D_w = a_0$ and $D_{lb} = D_{rb} = 3a_0$. The solid, dashed and dot-dashed curves represent $z_0 = 0$, $z_0 = -0.5D_w$ and $z_0 = 0.5D$, respectively.

change in binding energy with well width is more sensitive to the impurity position and Al concentration than the barrier widths, especially in asymmetric well structures where the barrier widths and/or barrier heights differ. The binding energy as a function of the impurity position in symmetric and asymmetric structures behaves like a map of the spatial distribution of the ground state wave function of the electron. It is also found that the influence on the binding energy from the Al concentration of the left barrier is more obvious than that of the right barrier.

References

[1] Oliveira L E. Spatially dependent screening calculation of binding energies of hydrogenic impurity states in GaAs–$Ga_{1-x}Al_xAs$ quantum wells. Phys Rev B, 1988, 38: 10641
[2] Zhao G J, Liang X X, Ban S L. Binding energies of donors in quantum wells under hydrostatic pressure. Phys Lett A, 2003, 319: 191
[3] Wen Shumin, Ban Shiliang. Screening influence on binding energies of donors in quantum wells with finite barriers under hydrostatic pressure. Chinese Journal of Semiconductors, 2006, 27: 63
[4] Wen Shumin, Ban Shiliang. Influence of polaronic effect on binding energies of donors in quantum wells with finite barriers under hydrostatic pressure. Chinese Journal of Semiconductors, 2007, 28: 848
[5] Oliveira L E, López-Gondar J. Acceptor-related photoluminescence study in GaAs/$Ga_{1-x}Al_xAs$ quantum wells. Phys Rev B, 1990, 41: 3719
[6] Latgé A, Porras-Montenegro N, de Dios-Leyva M, et al. Theoretical calculation of the miniband-to-acceptor magnetoluminescence of semiconductor superlattices. J Appl Phys, 1997, 81: 6234
[7] Shen Z J, Yuan X Z, Shen G T, et al. Effect of the electron-surface-optical-phonon interaction on the impurity-state energies in a semiconductor quantum well. Phys Rev B, 1994, 49: 11035
[8] Baskoutas S, Terzis A F. Binding energy of hydrogenic impurity states in an inverse parabolic quantum well under electric field. Physica E, 2008, 40: 1367
[9] Safwan S A, Elmeshed N, Asmaa A S, et al. Theoretical study of positive and negative donor impurity in quantum dot, quantum

well limit and quantum wire limit. Physica B, 2010, 405: 586
[10] Morel A, Lefebvre P, Taliercio T, et al. Donor binding energies in group III-nitride-based quantum wells: influence of internal electric fields. Mater Sci Eng B, 2001, 82: 221
[11] Liu D, Shi J J, Butcher K S A. Impurity bound polaron in wurtzite GaN/AlN quantum wells: the interface optical-phonon and the built-in electric field effects. Superlattices and Microstructures, 2006, 40: 180
[12] Zhu Y H, Shi J J. Donor binding energies in group III-nitride-based quantum wells: influence of internal electric fields. Physica E, 2009, 41: 746
[13] Lepkowski S P, Teisseyre H, Suski T, et al. Piezoelectric field and its influence on the pressure behavior of the light emission from GaN/AlGaN strained quantum wells. Appl Phys Lett, 2001, 79: 1483
[14] Nardelli M B, Rapcewicz K, Bernholc J. Strain effects on the interface properties of nitride semiconductors. Phys Rev B, 1997, 55: R7323
[15] Lepkowski S P. Nonlinear elasticity effect in group III-nitride quantum heterostructures: *ab initio* calculations. Phys Rev B, 2007, 75: 195303
[16] Wagner J M, Bechstedt F. Properties of strained wurtzite GaN and AlN: *ab initio* studies. Phys Rev B, 2002, 66: 115202
[17] Duan Y F, Li J B, Li S S, et al. Elasticity, band-gap bowing, and polarization of $Al_xGa_{1-x}N$ alloys. J Appl Phys, 2008, 103: 023705
[18] Wu J Q. When group-III nitrides go infrared: new properties and perspectives. J Appl Phys, 2009, 106: 011101